

## Spin States of $C_{60}^{3-}$ and $C_{120}O^{n-}$ ( $n = 2, 3, 4$ ) Anions Using Electron Spin Transient Nutation Spectroscopy

Simon C. Drew,<sup>\*,†,§</sup> John F. Boas,<sup>†</sup> John R. Pilbrow,<sup>†</sup> Peter D. W. Boyd,<sup>‡</sup> Parimal Paul,<sup>||,⊥</sup> and Christopher A. Reed<sup>||</sup>

*School of Physics and Materials Engineering, Building 27, Monash University, Victoria 3800, Australia, Department of Chemistry, University of Auckland, New Zealand Private Bag 92019, Auckland, New Zealand, and Department of Chemistry, University of California, Riverside, California 92521-0403*

*Received: June 10, 2003; In Final Form: July 22, 2003*

Electron spin transient nutation (ESTN) experiments show that the spin multiplicity of the ground state of  $C_{60}^{3-}$  in frozen solution is a doublet with  $S = 1/2$ . In purified samples, there is no evidence for excited states or other species with higher multiplicity. In the anions of  $C_{120}O^{n-}$  ( $n = 2, 3, 4$ ), where the CW EPR experiments have shown that a mixture of species is present, ESTN experiments confirm that a doublet with  $S = 1/2$  is associated with the 3- anion and triplets with  $S = 1$  are associated with the 2- and 4- anions. A weak nutation peak attributable to  $m_s = -1/2 \leftrightarrow 1/2$  transitions within a quartet state may arise from association of anions with spins of  $1/2$  and 1 in solute aggregates.

### Introduction

The observation of cooperative phenomena such as ferromagnetism<sup>1</sup> and superconductivity<sup>2</sup> in solid-state salts of the fullerene  $C_{60}$  has given impetus to extensive studies of the electronic properties of discrete fulleride anions. Molecular orbital calculations place a triply degenerate  $t_{1u}$  state as the LUMO, approximately 2 eV above the HOMO.<sup>3</sup> Thus, the simple expectation is that the addition of electrons to  $C_{60}$  will result in anions whose ground-state multiplicity follows Hund's rule, namely, the maximum multiplicity allowed by the Pauli principle. On this basis, the  $C_{60}^{3-}$  anion is expected to have a ground quartet state with spin  $S = 3/2$ .

The experimental evidence that this is not the case, and that the orbital degeneracy is removed to give a ground state with  $S = 1/2$ , is dependent on the interpretation of EPR spectra. The EPR observations have been reviewed by Eaton and Eaton<sup>4</sup> and more recently, by Reed and Bolskar.<sup>5</sup> The consensus view is that in frozen solution, the spectra of  $C_{60}^{3-}$  anions consist of a "broad line" whose width is variously reported as being in the range from 15 to 35 G, upon which is superimposed a "spike" of width 2–5 G. The shape and relative intensities of the broad line and the spike have been shown to depend not only on sample preparation but also on a variety of experimental conditions, such as temperature, freezing rate, microwave (mw) power, and magnetic field modulation amplitude. The influence of some of these factors on the spectra has been described elsewhere<sup>6,7</sup> and will be discussed more fully in a forthcoming publication.<sup>8</sup>

There has been debate as to whether the broad line and the spike are completely distinct species or whether circumstances

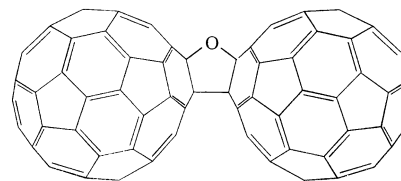


**Figure 1.** Structure of the dimeric fullerene  $C_{120}O$ .

exist where part or all of the resonant absorption of the spike contributes to that of the broad line.<sup>4,5,7</sup> However, recent EPR experiments by some of us, making use of samples of highly purified  $C_{60}$  and  $C_{120}O$  (Figure 1) prepared under anaerobic conditions, have shown that the broad line is due to  $C_{60}^{3-}$  itself and that the spike is due to  $C_{120}O$  impurities from the exposure of  $C_{60}$  to trace amounts of oxygen.<sup>9,9b</sup> The picture that emerges is that the broad line, due to an  $S = 1/2$  spin doublet, is the true resonance of  $C_{60}^{3-}$ , that the spike is due to a spin doublet from  $C_{120}O^{n-}$  with  $n = \text{odd}$ , and that the satellite lines observed in frozen solutions are due to the  $m_s = 0 \leftrightarrow \pm 1$  transitions of a triplet state from  $C_{120}O^{n-}$  with  $n = \text{even}$ . From this, it is deduced that the ground-state spin multiplicities of  $C_{60}^{n-}$  for  $n = 1, 2$ , and 3 are  $1/2, 0$ , and  $1/2$ , respectively, and those of  $C_{120}O^{n-}$  for  $n = 1, 2, 3, 4$ , and 5 are  $1/2, 1, 1/2, 1$ , and  $1/2$ , respectively. Hund's rule is not followed because the orbital degeneracy is removed by Jahn–Teller distortions.<sup>10</sup>

However, CW EPR measurements and simulations are unable to completely distinguish between the various possibilities where resonances from different species and different spin multiplicities overlap. First, both the spike and the broad line of  $C_{60}^{3-}$  could result from the  $m_s = -1/2 \leftrightarrow +1/2$  transitions within a spin quartet state rather than within a spin doublet. Second, the central line observed for the  $C_{120}O^{n-}$  mixture could arise, at least in part, from the  $m_s = -1/2 \leftrightarrow +1/2$  transitions within a spin quartet state of  $C_{120}O^{3-}$  and the various satellite pairs arise from the associated  $m_s = \pm 3/2 \leftrightarrow \pm 1/2$  transitions.

Electron spin transient nutation (ESTN) spectroscopy is capable of disentangling overlapping resonances and of distin-

\* Corresponding author. Tel: +61-7-3365-4237; fax: + 61-7-3365-3833; e-mail: simon.drew@cmr.uq.edu.au.

<sup>†</sup> Monash University.

<sup>‡</sup> University of Auckland.

<sup>||</sup> University of California.

<sup>§</sup> Present address: Centre for Magnetic Resonance, University of Queensland, St Lucia, QLD 4072.

<sup>⊥</sup> Present address: Central Salt and Marine Chemicals Research Institute, Bhavnagar, India.

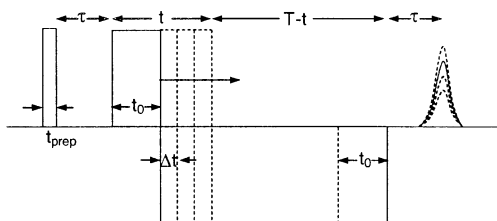


**Figure 2.** The PEANUT pulse sequence. The first pulse selects a window of spins and incrementing the phase boundary of the composite nutation pulse leads to the creation of a rotary echo at time  $t = T/2$ . The second part of the composite nutation pulse is  $180^\circ$  out of phase with respect to the other pulses.

guishing different spin states.<sup>11,12</sup> The ESTN spectroscopy of  $C_{60}^{3-}$  has been performed by Candida et al.<sup>13</sup> and the results interpreted as showing that the ground state of  $C_{60}^{3-}$  was  $S = 3/2$ . Because this is contrary to the conclusions of most other workers, we decided to perform ESTN measurements on well-purified samples prepared as described by Paul et al.<sup>9</sup> The ESTN measurements reported in this paper were performed using the PEANUT pulse sequence (phase inverted echo amplitude nutation).<sup>14</sup> This has the advantage that all echoes are detected at the same time, thereby minimizing loss of resolution because of relaxation broadening, as well as minimizing distortions arising from spectrometer downtime.

## Experimental Section

**Sample Preparation.** Samples were prepared at the University of California, Riverside as described earlier<sup>9</sup> and air-couriered to Monash University in dry ice to minimize the effects of aging. They were then stored at  $-20^\circ\text{C}$  prior to use.

**CW EPR.** EPR experiments were carried out with a Bruker ESP380FT/CW X-Band EPR spectrometer at Monash University. CW experiments were carried out both with a standard rectangular  $TE_{012}$  cavity and a Bruker ER 4118 cylindrical dielectric resonator. Temperatures of 77 K were achieved with a Bruker liquid nitrogen dewar and from  $\sim 100$  to  $\sim 160$  K using a Bruker Nitrogen Flow Cryostat fitted to the rectangular cavity. Temperatures from 2.7 K to approximately 175 K were achieved with the dielectric resonator inserted in an Oxford Instruments CF935 cryostat. Microwave frequencies were measured with an EIP Microwave 548A frequency counter.

The  $g$ -factors were determined with reference to the  $F^+$  line in CaO, which has a  $g$ -factor  $= 2.0001 \pm 0.0002$ .<sup>15</sup> Relative to the  $F^+$  line, the  $g$ -factor for DPPH was 2.0037 with an estimated uncertainty of  $\pm 0.0003$ , the same as the published value.<sup>16</sup>

**Pulsed EPR.** Pulsed EPR experiments were carried out at temperatures ranging from approximately 2.5–100 K using the ESP380E spectrometer fitted with the dielectric resonator and a 1 kW TWT amplifier. Echo-detected EPR (ED-EPR) spectra were acquired by recording the peak amplitude of a Hahn echo (obtained using the pulse sequence  $\pi/2-\Delta-\pi-\Delta$ -echo) as a function of magnetic field.<sup>17</sup>

The ESTN experiments used the PEANUT pulse sequence<sup>14</sup> shown in Figure 2. This consisted of a  $t_{\text{prep}} = 32$  ns preparation pulse, a free evolution period  $\tau$ , and a composite nutation pulse of duration  $T$  and power equal to the preparation pulse.<sup>18</sup> The precise microwave field at the sample depended not only on the high power attenuation setting but also on the loading of the resonator arising from sample positioning. The sampling digitizer was incremented by 16 ns for each  $\Delta t = 8$  ns increment of the phase-inversion point so that the oscillation frequency of the doubly nutating rotary echo appeared at the single nutation frequency  $\omega_{\text{TN}}$ . Data manipulation consisted of the subtraction

of the spin-locked echo contribution with a cubic polynomial fit, apodization with a Gaussian window function to isolate the rotary echo from the unrefocused contributions near  $t = 0$  and  $t = T$ , zero filling, and magnitude FFT calculation.

One-dimensional PEANUT experiments were carried out at a discrete number of magnetic field locations, corresponding to the prominent features in the ED-EPR spectrum. Following Stoll,<sup>19</sup> the 1D PEANUT spectra were symmetrized to reduce line widths and minimize artifacts. However, symmetrization can produce misleading results if the field is not close to one of the canonical orientations of the resonance in question, as discussed below. In some cases, the nutation spectra were signal averaged to obtain improved signal-to-noise ratios. Two-dimensional PEANUT experiments were performed by incrementing the magnetic field across the spectral region of interest.

For all pulsed experiments, the number of shots per loop was typically 10–50, with a repetition rate about a few hundred microseconds. All pulse lengths and experimental conditions are reported in detail later with the relevant results.

**Interpretation of Nutation Spectra.** Provided that the microwave field strength is such that only a single transition of the spin system is excited, the nutation frequency of the spin magnetization is given by the matrix element of the operator  $S_x$  by

$$\omega_{\text{TN}}(m_s \leftrightarrow m_s') = \omega_1 [S(S+1) - m_s m_s']^{1/2} \quad (1)$$

where

$$\omega_1 = g_1 \beta_e B_1 / \hbar = \gamma B_1 \quad (2)$$

$B_1$  is the magnitude of the microwave magnetic field,  $g_1$  is the  $g$ -factor along the direction of  $B_1$ , and  $m_s' = m_s - 1$  for allowed transitions. The multiplicity of the spin states corresponding to each of the features of the CW EPR spectrum can then be assigned by comparing the ratios of the frequencies of the peaks in the nutation spectra obtained at the fields of these features.<sup>19</sup> Thus, it is not necessary to know the precise strength of the microwave magnetic field  $\omega_1$  to assign spin multiplicities.

Equation 1 only applies when a single transition of the fine structure spectrum is excited.<sup>20</sup> This condition may be expressed as  $\omega_1 \ll |D|$  where  $D$  is the magnitude of the fine structure splitting. When  $\omega_1 \gg |D|$ , all spins experience the same effective mw field (i.e.,  $B_{\text{eff}} \approx B_1$ ) and hence have the same transition probability and nutation frequency. When  $\omega_1 \sim |D|$ , a range of nutation frequencies will result and the interpretation is no longer straightforward.

## Results and Discussion

**CW EPR Spectroscopy of  $C_{60}^{3-}$ .** The spectra of samples of  $[\text{Na}(\text{dibenzo-8-crown-6})]_3\text{C}_{60}$  in a 1:2 mixture of DMSO and THF were obtained at temperatures between 2.3 and 170 K. The spectra were consistent with those obtained by Paul et al.<sup>9</sup> with the same spectrometer settings of 5.7 mW microwave power and 5 G 100 kHz modulation amplitude. At lower powers and modulation amplitudes, the same two resonant features as reported by other authors could be discerned (see refs 4 and 5), namely, a resonance whose peak-to-peak derivative width varied between approximately 13 and 35 G and  $g$ -value  $\sim 2.0020$  upon which was superimposed a narrower resonance of width between 3 and 5 G and  $g$ -value  $\sim 2.0010$ . These features are referred to as the “broad line” and the “spike”, respectively. Representative spectra are shown in Figure 3. Because the spike saturates more readily than the broad line, it is better discerned in the low-power spectra. The low integrated intensity of the spike indicates

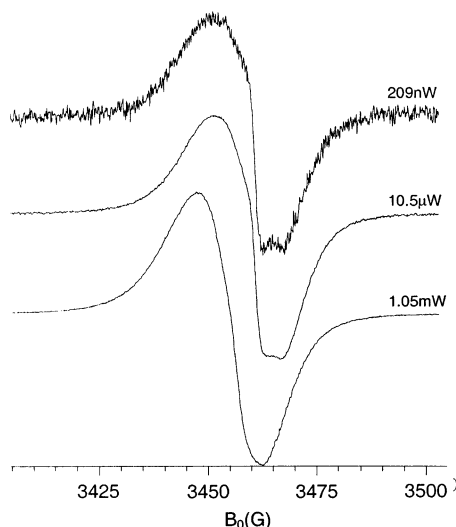


**Figure 3.** EPR spectra of  $C_{60}^{3-}$  at 2.5 K and microwave powers as shown. 100 kHz modulation amplitude 0.1 G; microwave frequency 9.692 GHz. Individual spectra have been adjusted to same peak height.

that the  $C_{60}^{3-}$  sample was almost free of  $C_{120}O$  impurity. The widths and relative intensities of the broad line and the spike are dependent on the sample temperature, the magnetic field modulation amplitude, the magnitude of the microwave magnetic field intensity,  $B_1$ , at the sample (which depends on the microwave power and the coupling to the resonant structure), and the rate at which the sample was cooled to the measurement temperature. The influence on the CW spectra of these factors and their reconciliation with the observations—but not necessarily the conclusions—of other workers will be discussed in a subsequent paper.<sup>8</sup> In summary, none of the spectra, under all conditions of observation, exhibited features other than those due to the broad line and the spike. There was no evidence for the temperature-dependent hysteresis effects observed by Candida et al.<sup>13</sup>

**Echo-Detected EPR of  $C_{60}^{3-}$ .** The ED-EPR spectra were obtained at 3.4 K with pulse lengths of 52 ns and 112 ns and a leading edge separation of 296 ns. A single slightly asymmetric resonance feature was observed. On differentiation, both the spike and the broad line could be resolved. As is the case with the CW spectrum, the spike is only a small component of the overall absorption, even though its narrowness leads to an impression of significant intensity when viewing the derivative spectrum.

**PEANUT Spectroscopy of  $C_{60}^{3-}$ .** The 2D ESTN spectrum at 4 K was acquired by incrementing the magnetic field at intervals of 1 G across the absorption spectrum. The initial duration  $t_0$  of the  $0^\circ$  phase component of the composite nutation pulse was 400 ns, as was the final duration of the  $180^\circ$  component. The free-evolution period  $\tau$  was 168 ns and the total duration  $T$  of the composite nutation pulse was 3192 ns (300 data points). The 2D-PEANUT spectrum is shown in Figure 4 and shows only a single nutation frequency. This establishes that only spin  $S = 1/2$  states are present and that therefore the broad line arises from an  $S = 1/2$  doublet ground state. Since the spike also has  $S = 1/2$ , it gives the same nutation frequency as the broad line. However, its presence is shown by the spin-lock projection depicted in Figure 5, where the broad line and the spike are clearly distinguished in the first derivative spectrum. The spin-lock projection is closely related to the ED-EPR spectrum and is derived from the 2D time domain data set by plotting the magnitude of the constant offset component of the nutation signal as a function of magnetic field.<sup>14</sup>

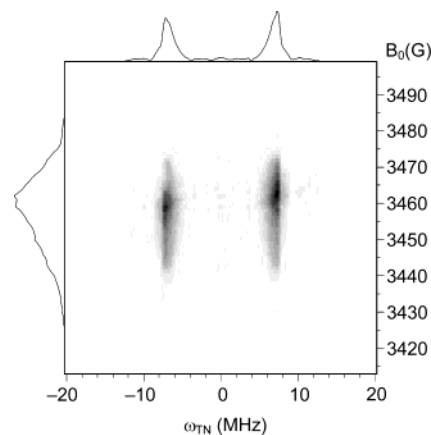


**Figure 4.** Linear density plot showing the nutation spectrum of  $C_{60}^{3-}$  at 4 K and 9.695 GHz as a function of static magnetic field, together with the sum projection along each dimension. There is evidence of incomplete removal of the  $\omega_{TN}$  signal arising from unfocused contributions near  $t = 0$  and  $t = T$ . There are also very weak and broad offset branches (see Discussion) from the narrow-line  $S = 1/2$  species (“spike”).

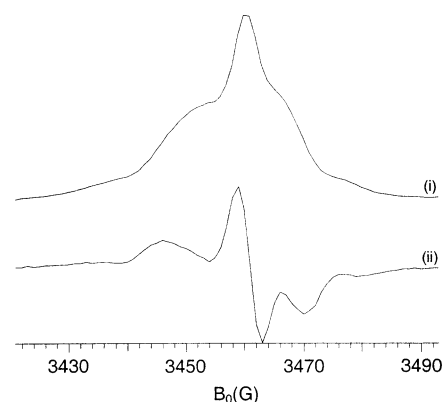


**Figure 5.** (i) “Spin-lock” projection spectrum for  $C_{60}^{3-}$ , derived from the data for Figure 4 as described in the text. (ii) First derivative of the spin-lock projection.

**CW EPR of  $C_{120}O^{n-}$ .** The CW EPR spectra of  $C_{120}O$  in solvent mixtures of 1:2:4 *o*-dichlorobenzene:dimethylsulphoxide:tetrahydrofuran after treatment with between 1 and 5 equivalents of reducing agent showed the same features as recorded by Paul et al.<sup>9</sup> when examined with the same spectrometer settings of 5 G magnetic field modulation amplitude, 5 mW microwave power, and at 100 K.

For the pulsed EPR experiments reported in this paper, we used samples of  $C_{120}O$  to which 3.2 equivalents of reducing agent had been added, written as  $C_{120}O;1:3.2$ . The CW EPR spectrum of these samples, recorded with a magnetic field modulation amplitude of 1 G, a microwave power of 10  $\mu$ W, and at a temperature of 100 K is shown in Figure 6. The lower modulation amplitude and microwave power gives a better resolution of the spectral components than reported in ref 10 but otherwise the features are identical.

Following Paul et al.,<sup>9</sup> we assign the strong line in the center of the spectrum (the central line) at  $g \sim 2.0010$  to  $C_{120}O^{3-}$ . The small satellite lines approximately 6 G either side of this line are assigned to the  $m_s = 0 \leftrightarrow \pm 1$  transitions within a triplet state arising as a consequence of the association of two  $C_{120}O^{3-}$  ions (the “powder triplet” of Paul et al.<sup>9</sup>). Such aggregation is the unavoidable result of freezing samples in the nonlossy solvent mixture required for adequate solubility. The satellite lines approximately 13 and 15 G either side of the central line are attributed to the perpendicular components of resonances

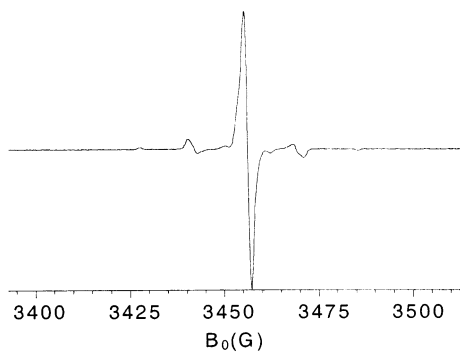


**Figure 6.** CW EPR spectrum at 100 K of  $C_{120}O$ ; 1:3.2. Microwave power  $10 \mu\text{W}$ ; 100 kHz modulation amplitude 1.05 G; microwave frequency 9.682 GHz.

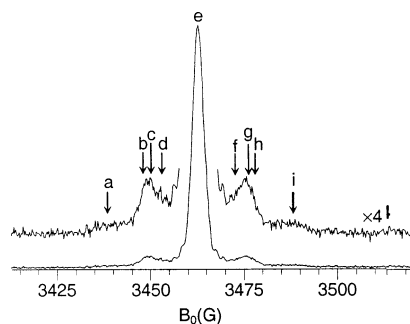


**Figure 7.** The ED-EPR spectrum of  $C_{120}O$ ; 1:3.2 at 100 K using the same sample as for Figure 6 and using pulse lengths of 56 ns and 112 ns with a leading edge separation of 200 ns. Microwave frequency 9.701 GHz. Average of 20 field scans. 1D nutation spectra using the PEANUT pulse sequence were acquired at magnetic field locations indicated **a**–**i**.

from the  $m_s = 0 \leftrightarrow \pm 1$  transitions of triplet states from  $C_{120}O^{2-}$  and  $C_{120}O^{4-}$  ions, respectively, (the “proper triplets” of Paul et al.<sup>9</sup>). Associated features approximately 30 G either side of the central line are assigned to the parallel components of these resonances.

The spectrum of Figure 6 thus shows evidence for the existence of  $C_{120}O^{2-}$ ,  $C_{120}O^{3-}$ , and  $C_{120}O^{4-}$ . The mixture of species arises inevitably from the closeness of the 2–/3– and 3–/4– reduction potentials of  $C_{120}O$  and the fact that these redox reactions are reversible. Although the central line has the greatest intensity in the first derivative spectrum of Figure 6, spectrum simulations and double integrations show that it represents only about 40% of the spin concentration. The resonances attributed to  $C_{120}O^{2-}$  and  $C_{120}O^{4-}$  represent about 25% each, respectively, and the resonances attributed to the powder triplet represent the remaining 10%. At around 100 K, the central line exhibits microwave power saturation behavior above about  $50 \mu\text{W}$  whereas the satellite features require greater than 1 mW. Thus, a true appreciation of the relative intensities of the resonances can only be gained at low powers.

The CW spectrum of  $C_{120}O$ ; 1:3.2 was also examined at 4 K. At this temperature, the relaxation times of all species are so long that only spectra reminiscent of fast passage effects<sup>21</sup> were observed, even at microwave powers of 200 nW and field sweep rates slower than 0.1 G per second. No features were observed at this temperature other than those connected to features in the spectrum of Figure 6.

**ED-EPR of  $C_{120}O^{n-}$ .** As shown in Figure 7, the ED-EPR spectrum with 3.2 equivalents of reducing agent exhibited a strong central feature at 3463 G and shoulders approximately equally spaced around the central resonance at fields of 3438, 3450, 3476, and 3488 G. These features can be related to features in the CW spectrum of Figure 6.

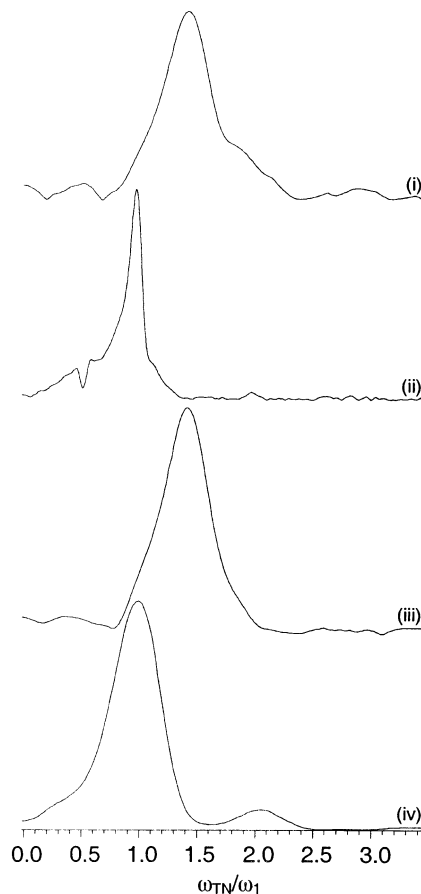


**Figure 8.** Normalized frequency domain nutation spectra for  $C_{120}O$ ; 1:3.2 at three of the magnetic field locations marked in Figure 7 [**c**, **e**, and **g**] obtained following Fourier transformation and manipulation as described in the text. (i) 100 K, field location **c**; (ii) 100 K field location **e**; (iii) 100 K, field location **g**; (iv) 60 K, field location **e**. The narrow hole at  $\omega_{TN}/2$  in (ii) has been experimentally observed in other  $S = 1/2$  systems, where it was attributed to artifacts introduced by data handling.<sup>14</sup> For the 100 K spectra,  $\omega_1/2\pi = 5.389$  MHz; for the 60 K spectrum  $\omega_1/2\pi = 8.946$  MHz.

**PEANUT Spectroscopy of  $C_{120}O^{n-}$ .** A 2D ESTN spectrum could not be obtained in this instance because of the inadequate signal-to-noise ratio. Therefore, signal-averaged 1D ESTN spectra were recorded at the magnetic field values **a**–**i** marked in Figure 7, corresponding to the prominent features of the ED-EPR spectrum. The initial duration,  $t_0$ , of the  $0^\circ$  phase component of the composite nutation pulse was 200 ns, as was the final duration of the  $180^\circ$  component. Representative nutation spectra are shown in Figure 8. At 100 K, the free-evolution period  $\tau$  was 168 ns and the total duration  $T$  of the composite nutation pulse was 3592 ns (400 data points) at center field (the position of the central line) and 1592 ns (150 data points) at all other magnetic field values. At 60 K,  $\tau = 112$  ns,  $t_0 = 200$  ns, and  $T = 1992$  ns (200 data points).

The nutation frequencies  $\omega_{TN}$  corresponding to fields **a**–**i** at 100 K are listed in Table 1. From Table 1, we see that the ratios of  $\omega_{TN}$  to  $\omega_1$  have a mean value of 1.43 ( $\pm 0.02$ ), which corresponds closely to the value of 1.414 expected for a spin doublet  $S = 1/2$  at center field and a spin triplet  $S = 1$  at the other fields.

At 100 K, there was inconclusive evidence for the existence of a quartet state ( $S = 3/2$ ) in the form of a very weak peak at a field corresponding to the center of the main line and with a nutation frequency of 10.73 MHz, approximately  $2\omega_1$ . Its intensity was at the noise level and corresponded to less than

**TABLE 1: Experimentally Observed Nutation Frequencies (100 K) at the Field Positions Indicated in Figure 7 and Their Ratio to that of the  $S = 1/2$  Species at the Center Field of 3463 G**

field marker	field (G)	$\omega_{TN}/2\pi$ (MHz)	$\omega_{TN}/\omega_1$
a	3438	7.729	1.43
b	3448	7.667	1.42
c	3450	7.790	1.45
d	3453	7.606	1.41
e	3463	5.389	1.00
f	3473	7.667	1.42
g	3476	7.729	1.43
h	3478	7.729	1.43
i	3488	7.667	1.42

**TABLE 2: Spin Hamiltonian Parameters Used in the 2D PEANUT Simulations of Figure 9**

species	SH parameter	value
$S = 1/2$	g	2.001
$S = 1$	$g_{\perp}$	2.0013
	$g_{\parallel}$	2.0019
	D	14.5 G
	E	0

5% of the peak intensity at  $\omega_1$ . The PEANUT experiment was repeated with another sample under the same conditions and the result was reproducible. The temperature was then reduced to 60 K to observe whether the nutation peak disappeared, as would have been expected if it originated from a thermally accessible excited state. Instead, we observed a significant increase in the signal-to-noise ratio of the  $2\omega_1$  peak, which was then easily discernible (Figure 8). Below about 40 K, the signal-to-noise ratio of all peaks rapidly diminished as the magnetization became saturated, even at very low repetition rates of the pulse sequence. This is consistent with the observation of rapid passage effects described above and is due to the increase in the spin-lattice relaxation times at low temperatures. The  $2\omega_1$  nutation peak implies the presence of a separate species possessing an  $S = 3/2$  ground state. The inability to observe any features in the CW spectrum which may be associated with  $S = 3/2$  species indicates that it is present in only small amounts.

**Simulations of 2D PEANUT Spectra.** The interpretation of PEANUT spectra is assisted by an investigation of the behavior of simulated spectra. 2D PEANUT spectra were simulated with a Fortran 90 program<sup>22</sup> using the first-order Hamiltonian<sup>23</sup>

$$\mathcal{H}_0 = g\beta_e B_0 S_z + \frac{D}{6}[3S_z^2 - S(S+1)]\left\{3\cos^2\theta - 1 + \frac{3E}{D}\sin^2\theta\cos 2\phi\right\} \quad (3)$$

which holds in the high-field approximation where the fine structure interactions are very much smaller than the Zeeman interaction. An isotropic inhomogeneous line width of  $\Gamma_{inh} = 5$  MHz was used in conjunction with the spin Hamiltonian parameters shown in Table 2. The value of  $B_1 = 1.926$  G used in the simulations corresponded to the experimental value of  $\omega_{TN}$  shown at position e in Figure 7 using eq 2. Other simulation parameters are listed in Figure 9.

The resolution of the time-domain spectra was 100 points in the nutation dimension and 80 points in the field dimension (1 G resolution). Powder averaging consisted of a summation over 100 equally spaced values of  $\cos\theta$  in the range  $[-1, 1]$ . The Gaussian inhomogeneous line shape, approximated by a truncated histogram, was accounted for by using a weighted summation over all resonance frequency offsets. The time-domain data from the simulations was processed using the

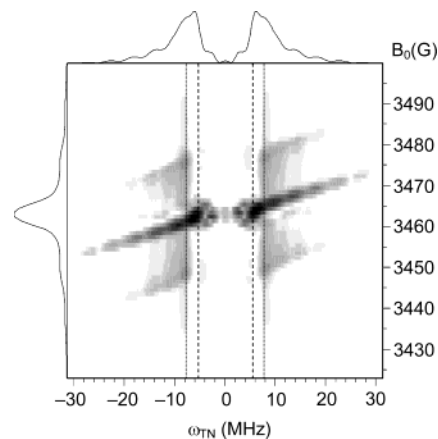


**Figure 9.** Logarithmic density plot showing a weighted summation of simulated 2D PEANUT spectra of  $S = 1/2$  and  $S = 1$  species, together with the sum projection along each dimension. The weighting was done in the time domain by making the spin-lock projections of the separate  $S = 1/2$  and  $S = 1$  spectra approximately the same intensity as their respective features in the ED-EPR spectrum of Figure 7. The Gaussian line width for each of the individual  $S = 1/2$  and  $S = 1$  simulations was approximated by a histogram containing 100 points and 50 points, respectively, truncated at  $\pm 3$  standard deviations. Simulation parameters: microwave frequency = 9.701 GHz,  $B_1 = 1.926$  G,  $t_{prep} = 32$  ns,  $\tau = 168$  ns,  $t_0 = 200$  ns,  $\Delta t = 8$  ns,  $T = 1192$  ns (100 data points),  $\Gamma_{inh} = 5$  MHz; spin Hamiltonian parameters are provided in Table 2. The dashed and dotted lines indicate the nutation frequencies expected from eq 1 for the  $S = 1/2$  and  $S = 1$  species, respectively.

Bruker Win-EPR software package in a fashion similar to the experimental data. An example is shown in Figure 9.

As well as exhibiting strong nutation peaks in the vicinity of 5.4 and 7.7 MHz, the 2D simulations show the presence of off-resonance  $0 \leftrightarrow \pm 1$  peaks. These manifest themselves as “offset branches”.<sup>18</sup> Caution must therefore be used when interpreting the experimental nutation spectra as these undesirable nutation peaks can confuse the identification of spin multiplicities. Such off-resonance effects were indeed observed in the experimental 1D PEANUT spectra of  $C_{120}O^{n-}$ , especially within  $\pm 5$ –6 G of the central resonance. This was the motivation for concentrating on the discrete locations a–i, because the off-resonance effects at these fields are expected to be minimized at these canonical orientations. The symmetrization of 1D nutation spectra at such fields further reduces the influence of such effects. However, symmetrization at fields other than those corresponding to canonical orientations can also lead to misleading interpretations. In the simulation of Figure 9 are the features at  $\approx \omega_{TN}/2$  in the vicinity of the canonical orientations, which arise because of incomplete removal of the rotary echo from unrefocused contributions near  $t = 0$  and  $t = T$ , prior to FFT.

Finally, we emphasize that Figure 9 is not an attempt to simulate the 2D spectrum of  $C_{120}O(1:3.2)$  but rather an attempt to illustrate the origin of some of the features encountered when 1D spectra are recorded at fields corresponding to other than canonical orientations.

## Conclusions

The ESTN experiments reported in this paper establish conclusively that the ground state of the spin system giving rise to the broad line in  $C_{60}^{3-}$  is a doublet with  $S = 1/2$ . There are no indications of spin states of higher multiplicity observed by ESTN at 2.6 K. The inability to observe any new resonances, as distinct from changes in line shape and intensity in the CW spectrum between 2.9 and 170 K and in the ED spectrum

between 2.6 and 100 K, implies that no excited states with spin multiplicity greater than  $1/2$  are significantly populated below about 170 K.

For the  $C_{120}O^{n-}$  systems investigated in this paper, the ESTN spectra show that the major species contributing to the central line of the CW spectrum is a spin doublet, that is,  $S = 1/2$ . The satellite features arising from  $C_{120}O^{2-}$  and  $C_{120}O^{4-}$  show peaks in the ESTN spectra corresponding only to spin triplets, that is,  $S = 1$ . This confirms the deductions of Paul et al.<sup>9</sup> on the basis of CW spectra. The inability to identify new features in the CW spectrum between 3.4 and 170 K (the melting point of the solutions) indicates that no states of higher multiplicity become populated in this temperature range. Furthermore, the spin singlet state ( $S = 0$ ) associated with the triplet because of the coupling of two  $S = 1/2$  systems must lie either above the triplet or be lower and separated from it by less than  $5\text{ cm}^{-1}$ .

Although we observed a nutation peak at a frequency corresponding to the  $-1/2 \leftrightarrow +1/2$  transition of a quartet state at field position corresponding to the center of the resonance attributed to  $C_{120}O^{3-}$ , its relative intensity indicates that it is only a minor species. The inability to observe any corresponding resonances in the CW spectrum and extra nutation peaks at  $\sqrt{3}\omega_1$ , a frequency corresponding to the  $\pm 3/2 \leftrightarrow \pm 1/2$  transitions, is consistent with this observation. Given that the powder triplet is attributed to the association of two  $C_{120}O^{3-}$  anions and that the sample used here contains a mixture of species, it seems reasonable to propose that a system with  $S = 3/2$  arises from the association of  $C_{120}O^{3-}$  (which has  $S = 1/2$ ) with either  $C_{120}O^{2-}$  or  $C_{120}O^{4-}$ , both of which have been shown to have  $S = 1$ .

As regards the central line, when examined under minimum conditions of modulation amplitude and microwave power, there appears to be no significant change in line width, line shape, intensity, or  $g$ -factor as a function of added reducing agent.<sup>9</sup> Thus, it appears that the central line observed from samples of  $C_{120}O^{n-}$  is always due to  $m_s = 1/2 \leftrightarrow -1/2$  transitions within a  $S = 1/2$  spin doublet. This doublet forms the ground state in all cases. There is no CW-EPR evidence for a contribution to the central line from higher multiplicity spin states.

In contrast to our results, which show no evidence for states other than doublet  $S = 1/2$  in  $C_{60}^{3-}$ , Candida et al.<sup>13</sup> have reported ESTN spectroscopic evidence for the existence of doublet and quartet states at center field and triplet and quartet states at the position of the so-called low field XY lines of the CW spectrum. However, as discussed by Paul et al.,<sup>9</sup> the CW spectra recorded at 90 K and presented as Figure 1 of Candida et al.<sup>13</sup> (cf. Figure 6 of this paper and Figure 8 of Paul et al.<sup>9</sup>) have the appearance of spectra arising from a mixture of  $C_{60}$  and  $C_{120}O$  anions. In particular, the XY lines appear to correspond to the satellite lines at around 3448 and 3478 G in our CW spectra of  $C_{120}O$  (1:3.2). The presence of  $C_{120}O$  anions in the sample of Candida et al.<sup>13</sup> leads to two possible explanations for the observation of a quartet state.

First, both  $C_{60}$  and  $C_{120}O$  anions have a marked tendency to associate when solutions are frozen.<sup>6,9</sup> It is possible for the quartet state observed by Candida et al.<sup>13</sup> to arise from associations between anions with spin  $S = 1/2$  and  $S = 1$  or between three anions, each with  $S = 1/2$ . We have similarly attributed our observation of a quartet state nutation peak at center field in  $C_{120}O$ (1:3.2) to the association of  $C_{120}O$  anions in solution on freezing. However, in our case, the quartet state appears to arise from a quite minor species.

Second, as described by Schweiger and Jeske,<sup>20</sup> if the magnitude of the  $B_1$  field is of the same order of magnitude as

the difference in frequency of two transitions with a level in common, the microwave excitation pulse is no longer transition selective. The mixing of the different transitions is then incomplete and nutation peaks can appear at frequencies other than those predicted by eq 1. In Candida et al.<sup>13</sup> the value of  $\omega_1/2\pi$  attributed to the  $S = 1/2$  species at  $g = 2$ , namely, 18.2 MHz, corresponds to a  $B_1$  field of  $\sim 6$  G. This is of the same order of magnitude as the zero-field splitting of the triplet state of the  $S = 1$  species, namely,  $|D| \sim 15$  G. Thus, the limiting condition of eq 1 no longer applies and the nutation peaks attributed to the quartet may be artifactual. By way of contrast, our measurements on  $C_{120}O$  (1:3.2) at 100 K yielded  $\omega_1/2\pi = 5.4$  MHz, corresponding to a field strength of  $B_1 = 1.9$  G, much less than the above value of  $D$ .

In summary, the complementary application of ESTN and CW EPR techniques has confirmed the conclusions of Paul et al.<sup>9</sup> regarding the spin state of  $C_{60}^{3-}$  and resolved uncertainties regarding the spin states of  $C_{120}O^{n-}$  ions in favor of those proposed.<sup>9</sup> Fulleride anions show a pronounced tendency to adopt low-spin states and although higher spin states may be thermally accessible, EPR spectroscopy on purified samples has so far failed to find convincing evidence for their existence.

**Acknowledgment.** We thank Drs. Dayong Sun and Kee-Chan Kim for assistance with the preparation of samples. This work was supported by NIH grant GM23851, the Marsden fund of New Zealand administered by The Royal Society of New Zealand (00-UOA-0303), and the School of Physics and Materials Engineering of Monash University. S.C.D. acknowledges the receipt of a Monash Graduate Scholarship during the course of this work.

## References and Notes

- (1) Allemand, P.-M.; Khemani, K. C.; Koch, U.; Wudl, F.; Holczer, K.; Donovan, G.; Grüner, G.; Thompson, J. D. *Science* **1991**, *253*, 301.
- (2) Hebard, A. F.; Rosseinsky, M. J.; Haddon, R. C.; Murphy, D. W.; Glarum, S. H.; Palstra, T. T. M.; Ramirez, A. P.; Kortan, A. R. *Nature* **1991**, *350*, 600.
- (3) Haddon, R. C.; Brus, L. E.; Raghavachari, K. *Chem. Phys. Lett.* **1986**, *125*, 450.
- (4) Eaton, S. S.; Eaton, G. R. *Appl. Magn. Reson.* **1996**, *11*, 155.
- (5) Reed, C. A.; Bolskar, R. D. *Chem. Rev.* **2000**, *100*, 1075.
- (6) Boas, J. F.; Drew, S. C.; Pilbrow, J. R.; Boyd, P. D. W.; Paul, P.; Sun, D.; Reed, C. A. *Proceedings of 27th Annual A & NZ IP condensed Matter and Materials Meeting (Wagga 2003)*; Cashion, J. D., Finlayson, T. R., Paganin, D. G., Smith, A. E., Troup, G. J., Eds.; www.aip.org.au; in press, 2003.
- (7) Eaton, S. S.; Kee, A.; Konda, R.; Eaton, G. R.; Trulove, P. C.; Carlin, R. T. *J. Phys. Chem.* **1996**, *100*, 6910.
- (8) Boas, J. F.; Drew, S. C.; Pilbrow, J. R.; Boyd, P. D. W.; Paul, P.; Sun, D.; Reed, C. A. manuscript in preparation, 2003.
- (9) Paul, P.; Kim, K.-Q.; Sun, D.; Boyd, P. D. W.; Reed, C. A. *J. Am. Chem. Soc.* **2002**, *124*, 4394. (9b) Other spikes can arise when an inappropriate solvent is used and reaction of  $C_{60}^{n-}$  with solvent (or solvent impurities) occurs. See Rapta, P.; Bartl, A.; Gromov, A.; Stasko, A.; Dunsch, L. *ChemPhysChem*, **2002**, *3*, 351.
- (10) Chancey, C. C.; O'Brien, M. C. M. *The Jahn Teller Effect in  $C_{60}$  and other Icosahedral Complexes*; Princeton University Press: 1997.
- (11) Astashkin, A. V.; Schweiger, A. *Chem. Phys. Lett.* **1990**, *174*, 595.
- (12) Schweiger, A.; Jeschke, G. *Principles of Pulse Electron Paramagnetic Resonance*; Oxford University Press: 2001; Chapter 14.
- (13) Candida, M.; Shohoji, B. L.; Luisa, M.; Franco, T. M. B.; Celina, M.; Lanzana, R. L. R.; Nakazawa, S.; Sato, K.; Shiomi, D.; Takui, T. *J. Am. Chem. Soc.* **2000**, *122*, 2962.
- (14) Stoll, S.; Jeschke, G.; Willer, M.; Schweiger, A. *J. Magn. Reson.* **1998**, *130*, 86.
- (15) Wertz, J. E.; Orton, J. W.; Auzins, P. *Discuss. Faraday Soc.* **1961**, *30*, 140.
- (16) Weil, J. A.; Bolton, J. R.; Wertz, J. E. *Electron Paramagnetic Resonance: Elementary Theory and Practical Applications*; Wiley-Interscience: New York, 1994; p 511.
- (17) Schweiger, A.; Jeschke, G. *Principles of Pulse Electron Paramagnetic Resonance*; Oxford University Press: 2001; p 183.

(18) The turn angle to be provided by the preparation pulse is nominally  $\pi/2$ . However, the requirement of a turn angle of  $\pi/2$  is obviously impossible to satisfy when species of differing  $S$  are present simultaneously. For a  $t_{\text{prep}} = 32$  ns and  $\omega_1 = 5.4$  MHz (as typically obtained in this paper) the nominal turn angle was  $\beta_0 = \omega_1 t_{\text{prep}} \sim \pi/3$ . The main purpose of the preparation pulse is therefore to provide a degree of orientation selectivity by exciting a frequency window of width  $\sim 1/t_{\text{prep}}$ . There are circumstances where an analogue of the PEANUT pulse sequence, without a preparation pulse, may be employed with advantage, see for example Tregenna-Piggot, P. L. W.; Noble, C. J.; Pilbrow, J. R. *J. Chem. Phys.* **2000**, *113*, 3289.

(19) Stoll, S. Diploma Thesis, TU Graz, 1996.

(20) Schweiger, A.; Jeschke, G. *Principles of Pulse Electron Paramagnetic Resonance*; Oxford University Press: 2001; p 429. An example of an analogous situation in NMR to one where  $\omega_1 \sim |D|$  is discussed by Kentgens, A. P. M.; Lemmens, J. J. M.; Guerts, F. M. M.; Veeman, W. S. *J. Magn. Reson.* **1987**, *71*, 62.

(21) Weger, M. *Bell Syst. Tech. J.* **1960**, *39*, 1013.

(22) Drew, S. C. Ph.D. Thesis, Monash University, 2002, Chapter 7.

(23) Pake, G. E.; Estle, S. C. *The Physical Principles of Electron Paramagnetic Resonance*, 2nd ed.; Benjamin: Reading, MA, 1973. Equations 5.29 and 5.36 have been combined and some symbols changed.